

FIG. 3. Chlorine NQR frequency spectra showing the satellites due to the chlorine ions which are nearest neighbors to the impurity. The intensities of the satellites are  $\sim 4\%$  that of the main line. (a) Spectrum at 77 K. (b) Spectrum at 298 K for the same number of averages.

the motion will have no appreciable effect on the

spectrum. The results suggest that the residence time for an  $H^+$  ion at an octahedral site in  $K_2OsCl_6$  at 298 K is short compared to  $10^{-3}$  sec but long compared to  $10^{-5}$  sec, that is, of the order of  $10^{-4}$  sec.

In conclusion, the work presented in this communication adds strong support to the speculation that the high electrical conductivity associated with  $K_2OsCl_6$  crystals is due to the presence of  $H^+$  ions which move through the lattice from one vacant fcc octahedral site to another.

<sup>1</sup>H. W. Willemsen, R. L. Armstrong, and P. P. M. Meincke, in *Proceedings of the International Conference on Fast Ion Transport in Solids, Lake Geneva, Wisconsin, May 1979*, edited by P. Vashishta *et al.* (North-Holland, Amsterdam, 1979), p. 413.

<sup>2</sup>The mass spectral analysis was carried out by the Chemistry and Materials Division of Atomic Energy of Canada Limited, Chalk River, Ontario K0J 1J0, Canada.

<sup>3</sup>R. W. G. Wyckoff, *Crystal Structures* (Interscience, New York, 1965), Vol. 3, p. 339.

<sup>4</sup>D. Nakamura and M. Kubo, *J. Phys. Chem.* **68**, 2986 (1964).

## Band-Tail Absorption in Hydrogenated Amorphous Silicon

Richard S. Crandall

RCA Laboratories, Princeton, New Jersey 08540

(Received 10 October 1979)

Measurements of the primary and secondary photocurrent for photon energies above 0.58 eV in  $a$ -Si:H solar-cell structures determine the absorption coefficient and give information about the density of valence-band-tail states as well as show that holes are mobile deep in the bandgap.

Photocurrent measurements are frequently used to detect defects that are in low concentrations. In hydrogenated amorphous silicon ( $a$ -Si:H) photocurrent measurements have been made using below-band-gap excitation to gain information about the band-tail states.<sup>1</sup> Since Ohmic contacts were used, they are *secondary* photocurrents<sup>2</sup> (SPC). Therefore, they are not a direct measure of the distribution of band-tail states because it is not known whether electrons or holes make the major contribution to the current. Because the photoconductive gain<sup>2</sup> is unknown, the absorption coefficient cannot be inferred from these measurements.

If the *primary* photocurrent<sup>2</sup> (PPC) is measured, then some of the above uncertainties are eliminated. Because a steady-state PPC (with use of blocking contacts) consists of equal numbers of electrons and holes, it is a direct measure of the number of excited electron-hole pairs. In an  $a$ -Si:H solar cell both PPC and SPC can be measured by the choice of the applied voltage. The reverse bias photocurrent is primary, and the far-forward-bias photocurrent is secondary.

In this Letter, I describe measurements of the PPC in  $a$ -Si:H, with photon energies down to 0.58 eV, that give the first determination of the absorption coefficient for weakly absorbing gap

states. Transient SPC measurements, used to determine the drift mobility of the majority carriers, show that photon absorption by gap states produces electrons in the same states as absorption by band states. This result leads to the conclusion that holes are mobile in gap states far above the valence band.

The structures are conventional Schottky-barrier solar cells.<sup>3</sup> Details of their production as well as the experiment will appear elsewhere.<sup>4</sup> The optical excitation source was a quartz iodine tungsten lamp whose output was dispersed by a grating monochromator. Filters at its output cut out unwanted orders and stray light. Transient SPC were measured using either pulsed solid-state lasers or a modulated cw He-Ne laser.

At high reverse bias the PPC is independent of voltage ensuring that all the excited carriers are collected. A typical current voltage curve is shown by the inset in Fig. 1. Since the reverse bias current is constant above about 3 V, the photocurrent ( $I$ ) can be related to the number of electron-hole pairs excited per second ( $N$ ) by the relation  $I = eN$ .

If the predominant optical absorption process is electron-hole pair production, then  $N$  determines the absorption coefficient ( $\alpha$ ). It is related to the number of incident photons ( $N_i$ ) by

$$N = N_i [1 - \rho \exp(-2\alpha l) - (1 - \rho) \exp(-\alpha l)], \quad (1)$$

where  $l$  is the film thickness and  $\rho$  the reflectivity at the back surface of the device. Since the structures have antireflection coatings, the contribution from front surface reflection can be omitted. In  $\alpha$ -Si:H solar cells the collection region is the region of high electric field or depletion region<sup>5</sup> because of the short minority-carrier diffusion length.<sup>6</sup> The undoped films are fully depleted.<sup>7</sup> The depletion width in doped films was determined from capacitance measurements under illumination.<sup>7</sup> The best evidence that the depletion width equals the sample thickness is that the photocurrent saturates in reverse bias.

In Fig. 1,  $\alpha$  determined from Eq. (1) is plotted versus photon energy ( $h\nu$ ). Curve  $b$  is for the sample in the inset. Curve  $a$  is for a  $\frac{1}{2}$ - $\mu\text{m}$ -thick Pt Schottky-barrier structure lightly doped with phosphorus ( $2 \times 10^{-4}$   $\text{PH}_3/\text{SiH}_4$  in the gas phase). Curve  $c$  is for a sample more heavily doped with phosphorus ( $2 \times 10^{-3}$   $\text{PH}_3/\text{SiH}_4$ ). It is an average through the interference fringes. The solid curve represents optical transmission measurements on a 6.6- $\mu\text{m}$ -thick undoped film prepared in the same way as the film used for curve  $b$ . The en-

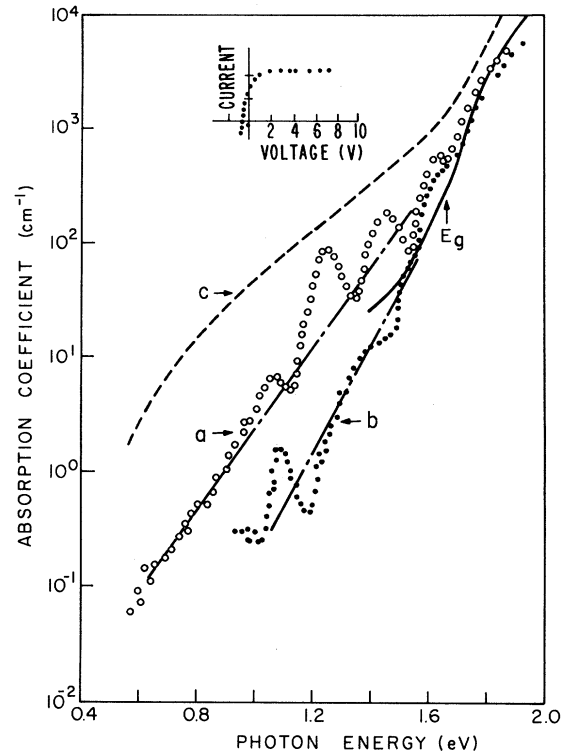


FIG. 1. The inset is photocurrent vs voltage applied to a Schottky-barrier  $\alpha$ -Si:H solar cell. Positive voltage is reverse bias. The photon energy is 1.49 eV and the temperature 250 K. The undoped film thickness is 0.6  $\mu\text{m}$ . The PPC is positive. The remainder of the figure is the absorption coefficient vs energy. The solid curve is the absorption coefficient measured on a thick film. Curve  $a$  is  $\alpha$  determined from the PPC on a 0.5- $\mu\text{m}$  doped film; curve  $b$ , on a 0.6- $\mu\text{m}$  undoped film; curve  $c$ , on a 1.6- $\mu\text{m}$  phosphorus-doped film.  $E_g$  is the optical gap.

ergy ( $E_g$ ) of the optical gap<sup>8</sup> is determined by plotting  $(\alpha h\nu)^{1/2}$  vs  $(h\nu - E_g)$ . The result is  $E_g = 1.65$  eV. The agreement between the two methods of measuring  $\alpha$  is seen to be satisfactory. The structure in the data obtained from the PPC is presumably caused by thin-film interference.

Additional information is obtained from the transient photocurrent when the solar cell is forward biased. The steady-state SPC density  $J_p$  is

$$J_p = eG\mu\tau V_F/l, \quad (2)$$

where  $V_F$  is the applied voltage minus the flat-band voltage (voltage at which the photocurrent changes sign). The mobility is  $\mu$ , the majority-carrier lifetime is  $\tau$ , and the number of free electron-hole pairs produced per unit time per unit volume is  $G$ . It can be determined if the re-

flectivity,  $\alpha$ , and the quantum efficiency for free carrier production can be measured. Since it is difficult to measure these parameters, it is much easier to determine  $G$  from the reverse-bias PPC. Since this current is a measure of the number of free electron-hole pairs,  $G = N/V$ , where  $V$  is the volume. Using Eq. (2) with  $N$  as obtained in Eq. (1), one can therefore determine the product  $\mu\tau$ .

Once the product  $\mu\tau$  has been determined the mobility can be found if  $\tau$  can be measured. One method is to measure the response time ( $\tau_R$ ) defined by<sup>9</sup>

$$\tau_R^{-1} = -[d \ln(J_p)/dt]_{t=0}. \quad (3)$$

However, in the presence of traps  $\tau_R$  will be longer than  $\tau$  by the ratio of trapped to free carriers. If  $\tau_R$  is then used in conjunction with the product  $\mu\tau$  to yield  $\mu$ , it will be the drift mobility ( $\mu_D$ ) of the majority carrier. Using different photon energies, one can then measure the product  $\mu\tau$  for excitations that put electrons and holes into states in the conduction and valence bands as well as into tail states. Then from a measurement of  $\tau_R$  one can determine  $\mu_D$  from the product  $\mu\tau$ .

The results of these measurements are shown in Table I. The surprising result is that  $\mu_D$  is virtually independent of excitation energy. The conclusion to be drawn from this is that the final state for majority-carrier electron is independent of the excitation energy. Additional support to this idea is given by the temperature dependence of  $\mu_D$ .<sup>4</sup> Its activation energy and magnitude are in reasonable agreement with that found by others.<sup>10</sup> The drift mobility has the same magnitude and temperature dependence for excitation above and below the band gap.

Apart from interference effects, the data in Fig. 1 can be represented by an Urbach tail to the band-edge optical absorption as is observed in other amorphous material.<sup>11</sup> This is shown by the broken lines drawn through the data points in curves *a* and *b*. One explanation is that it is caused by random electric fields broadening the

normally sharp absorption edge.<sup>11</sup> A similar explanation may apply here. However, a property of the Urbach tail is its temperature ( $T$ ) dependence of the form  $\alpha = c \exp(\gamma h\nu/kT)$  where  $\gamma$  and  $c$  are constants. Even though  $\alpha$  in Fig. 1 shows this exponential dependence on  $h\nu$  it does not exhibit the required temperature dependence.<sup>4</sup>

An alternate interpretation for the optical absorption is that it represents transitions between band-tail states whose densities have been measured by field effect and other means.<sup>12</sup> Roughly, the data can be represented by a density of states decreasing exponentially with energy away from the band edges.  $\alpha$  will be proportional to the product of these densities of states and the matrix element for the transition ( $B$ ) which is in general energy dependent. If we assume that  $B$  varies slowly with energy compared with the density of states, then the absorption coefficient can be shown to be of the form  $\alpha = C \exp(h\nu/E_v^0)$ .  $C$  is a constant and  $E_v^0$  is the characteristic energy of the density of states above the valence-band edge.<sup>13</sup> This expression for  $\alpha$  applies if  $E_v^0$  is larger than the corresponding quantity for conduction-band-tail states. This expression for  $\alpha$  shows that the important transitions are from states above the valence band to states in or near the conduction band. This is supported by the result that the majority-carrier drift mobility is independent of excitation energy. This argument does not depend on the detailed shape of the density of states but only that the density of states decreases more rapidly below the conduction-band edge than above the valence-band edge. The characteristic energies 0.1 and 0.09 eV for curves *a* and *b*, respectively, are larger than the measured values for the conduction-band density of states,<sup>12</sup> thus supporting our assumption. These values are also good representations of the field-effect density of states above the valence band.<sup>12</sup>

The above result, which depends on the matrix element for the optical transition changing slowly with energy, shows that  $\alpha$  maps out the density of valence-band-tail states. Figure 1 shows

TABLE I. Transport parameters measured at room temperature on undoped *a*-Si:H.  $J_{s.c.}$  is the short-circuit current.

Photon energy (eV)	$\tau_R$ ( $\mu$ sec)	$\mu_D$ ( $\text{cm}^2 \text{V}^{-1} \text{sec}^{-1}$ )	$J_{s.c.}$ (A)
1.99	$6 \pm 1$	$(7 \pm 2) \times 10^{-3}$	$7.5 \times 10^{-4}$
1.49	$7 \pm 1$	$(6 \pm 2) \times 10^{-3}$	$2 \times 10^{-4}$
0.99	$300 \pm 50$	$(8 \pm 5) \times 10^{-3}$	$1.6 \times 10^{-6}$

that phosphorus increases the valence-band-tail states. This is surprising since phosphorus is an  $n$ -type dopant.

The above argument that the holes are produced far above the valence band combined with the saturation with field of the primary photocurrent shows that holes are mobile deep in the band-tail states. Hopping conduction near midgap has been observed in  $a$ -Si:H (Ref. 14) with impurity densities on the order of those measured by field effect.<sup>12</sup> Even though the mobility of the holes in these deep states is low because of localization, the probability of their recombining with electrons is also low because of localization.

The author is indebted to H. Weakliem for making the optical absorption measurements as well as helpful advice and D. Carlson and E. Sabisky for supplying the samples. I am also indebted to I. Ladany and G. Olsen for supplying the injection lasers. This research was supported in part by RCA Laboratories and the U.S. Department of Energy under Contract No. ET-78-C-03-2219.

<sup>1</sup>P. G. LeComber, A. Madan, and W. E. Spear, in *Electronic and Structural Properties of Amorphous Semiconductors*, edited by P. G. LeComber and J. Mort (Academic, New York, 1973), p. 373; T. Suzuki, M. Hirose, S. Ogose, and Y. Osaka, *Phys. Status Sol-*

*idi* (a) **42**, 337 (1977).

<sup>2</sup>A. Rose, *RCA Rev.* **12**, 362 (1951).

<sup>3</sup>C. R. Wronski, D. E. Carlson, and R. E. Daniel, *Appl. Phys. Lett.* **29**, 602 (1976).

<sup>4</sup>R. S. Crandall, *Solar Cells* (to be published).

<sup>5</sup>C. R. Wronski, D. E. Carlson, and R. E. Daniel, and A. R. Triano, in *Proceedings of the IEEE International Electronic Devices Meeting*, Washington, D. C., December 1976 (unpublished), p. 75.

<sup>6</sup>D. L. Staebler, in *Proceedings of the Eighth International Conference on Amorphous and Liquid Semiconductors*, Cambridge, Massachusetts, 1979 (to be published).

<sup>7</sup>R. Williams and R. S. Crandall, *RCA Rev.* **40**, 371 (1979).

<sup>8</sup>J. Tauc, *Mater. Res. Bull.* **5**, 721 (1970).

<sup>9</sup>T. D. Moustakas and K. Weiser, *Phys. Rev. B* **12**, 2448 (1975).

<sup>10</sup>P. G. LeComber and W. E. Spear, *Phys. Rev. Lett.* **25**, 509 (1970); A. R. Moore, *Appl. Phys. Lett.* **31**, 695 (1977); W. Fuhs, M. Milleville, and J. Stuke, *Phys. Status Solidi* (b) **89**, 495 (1978).

<sup>11</sup>N. F. Mott, and E. A. Davis, *Electronic Processes in Non-Crystalline Materials* (Clarendon, Oxford, 1971), p. 238.

<sup>12</sup>W. E. Spear and P. G. LeComber, *Philos. Mag.* **33**, 935 (1976); G. H. Dohler and M. Hirose, in *Amorphous and Liquid Semiconductors*, edited by W. E. Spear (G. G. Stevenson Ltd., Dundee, 1977), p. 372.

<sup>13</sup>The density of states,  $N(E)$ , above the valence edge is represented by  $N(E) = A \exp(-E/E_v^0)$ .

<sup>14</sup>D. Allan, P. G. LeComber, and W. E. Spear, in *Amorphous and Liquid Semiconductors*, edited by W. E. Spear (G. G. Stevenson Ltd., Dundee, 1977), p. 323.

## Wake-Bound-Electron Contribution to Convoy-Electron Velocity Distributions: The Effect of the Ionic Field

Michael H. Day<sup>(a)</sup>

*Theoretical Physics Division, Atomic Energy Research Establishment Harwell, Didcot, Oxon OX11 0RA, England*

(Received 5 November 1979)

In the sudden approximation for surface penetration, a wake-bound electron emerges into vacuum with no net velocity relative to the ion it follows. After exit, the wake electron and ion interact via Coulomb attraction which introduces diffraction structure in the projectile-frame electron velocity distribution. Modeling of the detection process is done in order to compare with experimental results.

After a fast ion penetrates a thin solid (or gas) target, it emerges accompanied by electrons moving with velocities distributed near the velocity of the ion.<sup>1,2</sup> These "convoy" electrons<sup>3</sup> may be produced by three distinct mechanisms: (1) charge exchange from the atomic electrons of the target to the low-lying continuum states of

the ion<sup>4-7</sup>; (2) electron ejection from the ion's residual core due to interaction with the target constituents<sup>8,9</sup>; and, in the case of a solid target, (3) binding of electrons in the polarization wake of the ion which then follow the ion out of the solid.<sup>10-15</sup> Laubert *et al.*<sup>16</sup> observe differences in convoy-electron velocity distributions from solid